Hindawi
Mathematical Problems in Engineering
Volume 2022, Article ID 8449518, 11 pages
https://doi.org/10.1155/2022/8449518

Research Article

Machine Vision Nondestructive Inspection System Assisted by Industrial IoT Supervision Mechanism

Hairong Wang, Rong Lu, and Duo Yu

Department of Control Technology, Wuxi Institute of Technology, Wuxi, Jiangsu 214121, China

Correspondence should be addressed to Hairong Wang; wanghr@wxit.edu.cn

Received 7 February 2022; Revised 10 March 2022; Accepted 14 March 2022; Published 21 April 2022

Academic Editor: Gengxin Sun

This paper introduces the development status of machine vision nondestructive testing technology and industrial IoT supervision mechanism. The study designs and implements a machine vision nondestructive testing system from two aspects: construction of industrial IoT supervision and detection model, and optimization of machine vision nondestructive testing algorithm. In this paper, the random deployment of dynamic and static nodes is adopted. The coverage rate after random deployment and the moving distance of dynamic nodes are two necessary research parameters. To improve the initial coverage and optimize the mobile path of dynamic nodes, this paper proposes a mobile deployment optimization scheme based on the supervisory mechanism model of industrial IoT, which improves the traversal of the quantum genetic algorithm by improving the genetic variation rules, thus improving the initial deployment of the network. The optimized machine vision nondestructive detection algorithm is used for mobile path optimization from dynamic nodes to target locations. Simulation results show that a random deployment of 100 static nodes and 20 dynamic nodes in a 400 m × 400 m factory area works best with a coverage rate of 6.719% and an average movement distance of 23.47 m, and the movement path avoids the obstacle area. The average accuracy of the modified machine vision nondestructive testing system is 1.59% higher than that before the modification, and the average detection accuracy of the final experiment reaches 95.46%. Not only is the coverage rate better than that of the cellular structure-based dynamic node optimization scheme, but also the monitoring range of the plant tends to be more comprehensive in the actual deployment environment. Through the analysis of test results, the system achieves the monitoring and display of data on the one hand and provides a natural information access and interaction experience for IoT managers on the other hand, which meets the requirements of real time, accuracy, and stability of industrial IoT information data to a certain extent.

1. Introduction

With the rapid development of digitalization and networking in the industrial field, the industrial Internet of Things (IIoT), which relies on IoT technology for information sharing and intelligence, has come into being [1]. The IIoT fully integrates various information collection sensors and controllers with monitoring and sensing capabilities, as well as 5G, big data analysis, and artificial intelligence technologies to achieve ubiquitous sensing of all aspects of industrial production, resulting in a wide range of efficiency improvements in industrial manufacturing, significant decreases in the number of defective products, and large reductions in product resource consumption [2]. Finally, the traditional industry will be elevated to a new level. Smart devices and smart production have a positive impact on people's daily life, and the combination of IoT technology and the traditional design and manufacturing model of the smart industry also plays a positive role in industrial production, which is also called the industrial Internet of Things [3]. Compared with the traditional manufacturing model, real-time monitoring systems in the smart era continue to develop, which not only can promote the progress of production methods and production efficiency, but also effectively reduce the number of safety issues. Monitoring systems in intelligent machine vision nondestructive testing greenhouse have made corresponding development, but to avoid unnecessary waste of resources and casualties, monitoring systems in the industrial field have very broad application prospects [4].

To keep pace with the development of the times, it is obvious that the production methods of traditional manufacturing industries cannot meet the current market demand. While using information technology to improve the production methods, the management measures and safety facilities of factories should also be scientifically improved; otherwise, safety problems will occur [5]. Whether it is the working environment, the manufacturing equipment, or the specific operation of the employees in the factory, there are safety hazards in each link; in addition, whether the safety management department can find and investigate the safety hazards in time is a great test for them. Despite the advanced technology today, the monitoring system has entered daily life, but the shortcomings such as poor data integration, lack of system maintenance, and incomplete data records have seriously affected the normal operation of the monitoring system. In this situation, it is especially important to design and develop a complete digital monitoring system. The combination of industrial IoT and labor-intensive agroindustry is setting off a new revolution in machine vision NDT technology [6]. The notice issued by the State Council on the development plan of a new generation of artificial intelligence also clearly points out that, under the impetus of socioeconomic development and new technology theories, cross-border integration in various fields is needed to accelerate the intelligent upgrading of industries, in which the demand for establishing an integrated application of machine vision nondestructive intelligent supply chain is put forward in intelligent machine vision nondestructive testing. Industrial Internet of Things, as a branch of artificial intelligence, has obvious advantages in the application of vision, and applying industrial Internet of Things to machine vision nondestructive testing is a trend to improve the development of machine vision nondestructive testing in recent years [7]. In highly polluting industries such as chemical industry and light industry, it is necessary to support the establishment and improvement of an intelligent sewage monitoring system. It is necessary to realize the integrated application of intelligent sewage automatic monitoring devices, water quality data monitoring devices, and water quality parameter detectors and other equipment and implement key enterprises for sewage monitoring. Real-time monitoring, automatic alarming, and remote closure of sewage outlets are required to prevent the occurrence of sudden environmental pollution accidents.

This paper mainly takes the application of industrial Internet of Things (IoT) as the research background, combines industrial IoT and machine vision nondestructive testing technology by using the convenience of the mobile terminal, and proposes a set of mobile interactive system design schemes for controllable and displayable equipment data monitoring and machine vision nondestructive testing display [8]. The scheme combines the advantages of IoT intelligent technology and advanced machine vision technology and integrates them with the data collection monitoring and NDT system of industrial equipment, constituting a real-time, stable, convenient, and efficient mobile interactive system. In Section 1, the main work is to explain the research background of the paper and the significance of the development of machine vision NDT technology and to arrange the main contents of the paper. Section 2 aims to understand and introduce the status of relevant domestic and international research on industrial IoT and machine vision nondestructive monitoring. Section 3 describes the functional requirements and performance requirements of the machine vision nondestructive inspection system based on the industrial IoT. Based on these requirements, the overall scheme of the machine vision nondestructive inspection system is designed; a joint perception probability model that is more in line with the actual situation is adopted for the optimization of the IoT coverage of the mixed deployment of dynamic and static nodes and the dynamic node movement path; a joint perception probability model based on the industrial IoT is proposed; and a supervisory mechanism of machine vision nondestructive detection algorithm is used for IoT network node random deployment and mobile path optimization scheme, which not only utilizes the mobility of dynamic nodes to repair coverage voids but also achieves some results for dynamic nodes' mobile path optimization. Section 4 conducts experiments on the designed machine vision nondestructive inspection system based on the industrial IoT supervision mechanism, analyzes the experimental results, and compares them with the simulation conclusions. Section 5 first summarizes this paper, then analyzes the shortcomings of the existing system, points out the improvement direction, and lays the foundation for the subsequent research.

2. Key Technology

In the traditional industrial IoT, sensor devices are no longer able to meet the needs of the emerging industry under the high demand of society for industrial production and paradigm updates [9]. With the development of miniaturization and information intelligence in IoT, sensor development also tends to be more and more intelligent, which promotes the development of data acquisition technology in industrial IoT [10]. Dhiman B et al. [11] designed a multifrequency machine vision nondestructive MWM array sensor, and experiments showed that the sensor has good detection capability for fatigue damage of steel [11]. Khan S et al. designed a CODFCI sensor, which combined a detection coil with a high-resolution charge-coupled device to make a probe. The experiments showed that the probe has a good detection effect on various alloy surface defects [12]. Sahu C K et al. used wireless sensors to conduct some research on natural disasters of landslides and constructed a wireless sensor network for remote monitoring of landslides [13]. Once there is a possibility of landslides, the network will generate early warnings, which can make the lives of residents safe. To be guaranteed, a system that can remotely monitor the state of the machine is proposed, which contributes to the safety and reliability of the machine. From the status quo, we can know that both the industrial Internet of Things and the remote monitoring technology of equipment have penetrated the actual production and human daily life

unconsciously [14]. Regardless of the different monitoring technologies, their ultimate goal is to achieve network interoperability, make plans for the industrialization construction of key technologies and important development areas that need to be broken through in the field of the Internet of Things, and provide financial support for industrialization projects that meet the requirements. The technologies supported by the Internet of Things industry research and development include network transmission equipment and information processing products, including wireless sensor network equipment, communication modules based on TD-SCDMA technology, and massive information analysis and processing.

With the continuous development of semiconductor integrated circuits, microprocessor-based embedded devices will continue to develop in the direction of high speed, high reliability, and low cost, and their hardware resources are gradually enriched. Embedded machine vision system benefits from its advantages of small system scale and high integration and is widely used in application fields with high research value [15]. The execution efficiency of vision algorithms to a certain extent restricts the efficiency of many current machine vision systems, resulting in some computationally intensive vision systems that do not have high execution efficiency [16]. Sun Q et al. propose an anonymous aggregated encryption scheme that encrypts several different messages into a single ciphertext and sends them to multiple end users, each of whom decrypts the message using the decryption key they have to obtain the corresponding plaintext message, which effectively reduces the computational overhead in industrial IoT systems [17]. Tripathi M K et al. proposed elliptic curve-based privacy-preserving industrial IoT user authentication machine vision nondestructive testing considering the limited resources of smart device nodes in industrial IoT systems [18]. The scheme exploits the nature of elliptic curves to ensure the security of messages while effectively reducing the computational cost associated with authentication [19]. Wu C et al. proposed an efficient edge computing-based message authentication scheme to address the overhead problem of message authentication in industrial IoT [20]. In the process from the production of the product in industrial manufacturing to the sale of the product, it is usually necessary to track the product to deal with the recall of the product. For example, food manufacturing, as an application in the industrial Internet of Things, often needs to be aware of expiration dates.

The food in question is recalled. However, the use of cloud servers is not conducive to deployment in the production chain and sales chain of food. The framework based on edge computing can be applied in the food manufacturing industry. In their proposed scheme, the production and sales process of food is recorded by methods such as QR codes, so that the production and supply chain of products can be identified and tracked.

Fully dynamic nodes are deployed with high mobility, and coverage voids have more possibilities of being effectively covered. The scheme of dynamic nodes moving toward the center point of the void can effectively improve the coverage rate, and the neighboring nodes below the distance threshold move in the direction away from the center point of the void, which improves the redundant coverage problem of the nodes; however, the cost and difficulty of laying the Industrial Internet of Things with fully mobile nodes is high the overall energy consumption of the industrial IoT is too large, and there will be the problem of mobile path interference of dynamic nodes. The expansion model of industrial IoT machine vision nondestructive detection based on genetic algorithm designs the fitness function based on machine vision nondestructive detection response data, selects the good individuals among the new samples generated by crossover and mutation operations, finally expands the high-quality machine vision nondestructive detection samples after several evolutions, and uses the expanded high-quality machine vision nondestructive detection samples to train the hidden Markov-based machine. The parameters of the expanded high-quality machine vision NDT model are used to train the hidden Markov-based machine vision NDT detection model, which improves the accuracy of IIoT machine vision NDT detection. Finally, a highly automated and accurate IIoT sparse machine vision NDT inspection system is designed based on comparing the effect of the two models on IIoT machine vision NDT inspection, and the effect of other machine vision NDT inspection models on IIoT machine vision NDT inspection is experimentally compared to verify that the system has better detection effect on IIoT machine vision NDT inspection. The target detection algorithm based on deep learning is a nondestructive detection method. Based on the self-collected data set, an industrial Internet of Things supervision and detection algorithm model is constructed to detect the damage and nondestructive conditions of the appearance of apples. This paper summarizes the factors that can improve the accuracy of the network model through experiments and finally improves the accuracy of target detection by modifying the model parameters, expanding the data set, and using excellent feature extraction network model methods.

3. Research on Machine Vision Nondestructive Inspection System Based on Industrial IoT Supervision Mechanism

3.1. Industrial IoT Supervisory Detection Model Construction. The model in this paper mainly involves the coil in the probe, the model of the metal specimen to be measured, and the observation line. The center of the observation line is considered as the location of the giant magnetoresistance (GMR) sensor, and the change in the output signal of the sensor can be obtained by calculating and analyzing the change in the magnitude of the magnetic induction on the observation line. First, a 3D simulation project is created, and the solution type is set to eddy current; then, the model to be simulated is determined. Since this paper is concerned with the detection of defects on the surface of an aircraft, the target is identified as the detection of defects and cracks on the surface of an aluminum plate. A rectangular specimen of

50 cm × ∗ 50 cm × ∗ 0.5 cm is created in the blank project. The defects on the surface of the specimen can be detected by creating a separate rectangle in the project with the same size as the defects. After setting up the solution model, you need to set up the excitation source and solution domain for the solution model. The industrial IoT supervised inspection model is shown in Figure 1. Add a solver to the established model, and only modify the self-adaptive frequency of the solver to the size of the frequency that needs to be simulated. You can also use the frequency sweep function to perform sampling simulation with a certain step size for frequencies within a certain range. After using the function to check that the model is correct, start the analysis and calculation.

Select the excitation coil model, and profile it in direction to obtain two rectangles of the excitation coil cross section. Separate the two rectangles, keeping only one of the faces, and add current excitation to this face. Since the excitation coils wound with multiple layers of wires are modeled as equivalent to copper rings, the excitation is added by applying an equivalent current through the single wire current multiplied by the size of the coil turns. The observation line is added to the simulation results to obtain the magnetic induction intensity in a certain direction on the observation line. Place the observation line 1 mm above the monitoring object, allowing it to pass through the center of the coil and be perpendicular to the defect. Use the Field Calculator settings to solve for the magnetic induction distribution in the direction normal to the surface of the monitored object.

The excitation probe selected in this paper is a multi-turn placement coil, and the next analysis is calculated using (1) to obtain the magnitude of the magnetic field generated by the coil. The wavelength of the electromagnetic wave is shown in (1), where δ is the electromagnetic wave propagation velocity of 4×105 m/s and $f(x)$ is the excitation frequency experiments used in the frequency range of 0.2–2.5 kHz. From this, we can obtain the wavelength range of 1×105 to 4×105 mm. Generally, the magnitude of the distance to the metal sample measured by the eddy current probe is in the order of millimeters, which is negligible compared with the wavelength.

$$F(x) = \left(\sum_{i=1}^{N} x_i * \delta \right) * f(x). \tag{1}$$

The instantaneous value of the electromagnetic field is calculated using the static field calculation method. According to law, the magnetic induction generated by a single-turn wire on its axis is shown in (2) where $E(x)$ is the magnitude of the magnetic induction at that point; η_0 is the magnetic permeability in a vacuum, $3\pi x10^{-7}$, $3\pi x10^{-7}$; I is the magnitude of the current through the circular wire; x is the vertical distance from the point on the axis to the plane of the coil; and R is the radius of the circular wire.

$$E(x) = \frac{\eta_0 * I * R^2}{3\left(x^2 + R^2\right)^{2/3}}. \tag{2}$$

The magnetic field of an excitation coil at a point on the perimeter line can be considered as the superposition of the magnetic inductance strength of multiple single-turn coils at that point. Let the number of turns of the excitation coil be M. Then, the current density on the excitation coil is as follows:

$$\forall(x) = \frac{M}{R_j - R_i} * \frac{F(x)}{E(x)}. \tag{3}$$

The magnitude of magnetic induction intensity at any point on the central axis of the excitation coil is shown in (4). From (4), it can be seen that the magnitude of magnetic induction at any point on the axis of the eddy current detection probe is related to the frequency and size of the excitation signal and the inner and outer diameter, and the number of turns and thickness of the excitation coil; the greater the excitation current, the greater the magnetic induction; the more the turns of the coil, the greater the magnetic induction. Therefore, in the simulation design, the above parameters should be modified so that the designed excitation coil can produce the maximum magnetic induction strength under the same conditions.

$$E(x) = \left[(x + e(x) \log \frac{R_i + \sqrt{R_i^2 + x + e(x)}}{R_j + \sqrt{R_j^2 + x + e(x)}} \right] * \frac{\eta_0 * M * I(x)}{3\left(R_j - R_i\right) * e(x)}. \tag{4}$$

The number of turns of a coil can be considered as the quotient of the total volume of a multi-turn coil and the volume of a single-turn coil as shown in (5), where $M(x)$ is the number of turns of the coil; n is the width of the coil, numerically equal to the difference between the inner and outer radius of the coil; m is the height of the coil; and d is the diameter of the coil. Since the diameter of the enameled wire D is fixed, it can be found from (5) that the coil height m and width n are inversely proportional when the number of turns of the coil is constant.

$$M(x) = \frac{3 * m * n}{4\lambda * \pi * D^2} \ln \sum_{i=1}^{M} e(x_i). \tag{5}$$

3.2. Machine Vision NDT Algorithm Optimization. In this paper, the fitness function is used to evaluate the merit of machine vision nondestructive inspection data. In each iteration, the updated data is sent to the industrial IoT test network, the response results are recorded, and the min and max are updated; then, the value of the fitness function is calculated, and the individual optimum of the particle and the global optimum of the whole population are updated according to their values so that the particles of the population are approximated to the most. After several iterations, we finally obtain a certain number of normal returns. In the data expansion model, the fitness function is not known; combined with the actual application scenario, the fitness function is designed as the distance between the machine vision nondestructive detection field and the current minimum value $\min(L(x))$, $\min(L(x))$; in the machine vision nondestructive detection data expansion model, the equation of the fitness function is as in (6).

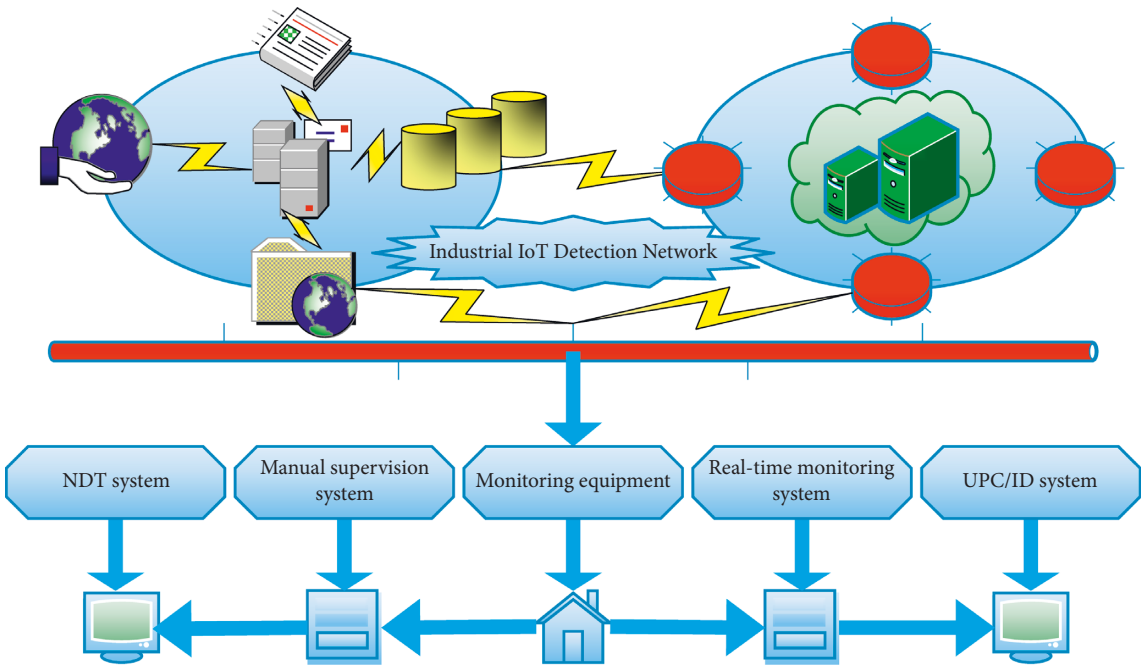

Figure 1: Industrial IoT supervisory inspection model.

Among them, x_i is the value of the field that needs to be optimized in the i-th abnormal return data and *min* is the minimum value of the field in the normal return data obtained in the data preprocessing stage; the fitness function $H(x)$ represents the current distance between the first data and $\min(L(x))$, $\min(L(x))$; the smaller the distance, the more optimal the particle.

$$H(x) = \sum_{i=1}^{N} (x_i - \min(L(x)). \tag{6}$$

The maximum likelihood probability estimation of the hidden state sequence in the machine vision NDT inspection model designed in this paper represents the best prediction of the observed sequence, so our goal is to find the state sequence with the maximum likelihood probability, and the genetic-based Viterbi algorithm is used in this paper to estimate the state sequence with the maximum likelihood probability. In this paper, we introduce the parameters J and K and define the probability maximum in all individual paths $(k_1, k_2 \cdots k_x)$ of the hidden state at moment t as follows:

$$\begin{cases} J(x) = \max(k_1, k_2 \cdots k_{x-1}) * H(k_1, k_2 \cdots k_x | \kappa), \\ x \subseteq [1, 2, \cdots M]. \end{cases} \tag{7}$$

The recurrence equation for the variables can be obtained as follows:

$$J(x+1) = J(x) + H(k_{x+1} | \kappa). \tag{8}$$

The previous state is $J(x)$ recorded $K(x)$ as shown in (9). When $x - i = k_i$ the algorithm stops. Finally, the hidden state sequence $\{i_1, i_2 \cdots i_k\}$ with maximum likelihood probability is obtained, which is the best format for the unknown industrial IoT machine vision nondestructive field.

$$K(x) = \tan \sum_{i=1}^{M} J(x-1) * H(i, \kappa) * J(x) * H(i+1, \kappa). \tag{9}$$

The device does not return a response to the request, and no response includes request format errors and so on. Finally, based on the returned response, the adaptation function is designed with the following equation:

$$Q(t, \kappa) = \begin{cases} t-1, & x \succ M, \\ t, & x = M, , \\ t+1, & x \prec M, \end{cases} \quad M = \sqrt{X^2 + Y^2 + Z^2}. \tag{10}$$

In this paper, the responses returned by machine vision nondestructive testing are divided into three different levels (the level represents the quality of machine vision nondestructive testing samples; the higher the level, the higher the quality of machine vision nondestructive testing samples). The levels are X, Y, and Z in descending order, which represent the fitness value of the test sample when a normal response is returned, when an abnormal response is returned, and when no response is returned. The specific values of the parameters depend on their quality and efficiency for the expansion of machine vision nondestructive testing and are constants; κ denotes the normal response set, M denotes the abnormal response set, and N denotes the no-response set. Since for this paper the data that can return normal responses are of high quality, this paper stipulates that the value of X is greater than the values of Y and Z, and the value of Y is greater than Z. To ensure the quality and efficiency of the machine vision NDT expansion, the specific

values of the parameters need to be taken through extensive experiments on the industrial IoT machine vision NDT.

$P(x)$ represents the speedup ratio of a parallel system, which is defined as the ratio of the single-computer computation time $P(t+1)$ to the multicomputer computation time $P(t)$ for parallel computing problems. The equation for calculating the speedup ratio under a fixed-size parallel system is shown in (11). P is the size of the parallel computing system. The tasks of the system are divided into two parts, serial and parallel. $q(x)$ and M correspond to and have $q(x)+M$, $q(x)+M$. It can be seen that increasing the percentage of parallel tasks can improve the speedup ratio of the system under a fixed system size.

$$P(x) = \frac{q(x)+M}{q(x)+M/P} * \sum_{i=1}^{N} x_i + \frac{P(t+1)}{P(t)}. \tag{11}$$

For practical physical problems, parallel computing is adopted to divide the physical problems into computational tasks and carry out the abstraction of the computational model. The parallel program is implemented in a computer language. The specific algorithm flow is shown in Figure 2. The core idea of parallel computing is to decompose a more complex computing problem into small computing units, then publish these computing units to run on a virtual parallel computer, and finally summarize the computing results. These computing tasks are generally performed by a computing program process of a computer on the network, the program processes can share information, and such a process can become a computing node. Computational tasks can be performed on the same computer in physical space or distributed among multiple computers.

3.3. Machine Vision Nondestructive Inspection System Design and Implementation. The website of the machine vision NDT system designed in this paper is divided into four functions: system login, data query, device management, and background management. To prevent the information and data in the system from being deleted or even being unrecoverable due to some mistakes, access to the background management module will not be opened to ordinary users. For the machine vision NDT system designed in this paper, real-time monitoring of data and historical query of data are the most basic functions. Data real-time detection can be intuitively seen in the designed real-time data monitoring interface of machine vision nondestructive temperature, speed, torque, pressure, and other data; users can query the past equipment data through the history query function. Firstly, set the period of the query, and then select the required equipment and data; you can get the data that the user needs. For example, if a new data stream is needed, the system user can add the corresponding industrial equipment to the equipment list; if a data stream no longer needs to be monitored, the system user can delete the corresponding equipment from the equipment list.

For visual inspection systems, to reduce the communication load caused by image transmission, a parallel computing structure of distributed storage can be used. Each computing node independently manages its computing, IO resources, etc., and each node is relatively independent and locally autonomous. The computing node only communicates with the master node and does not communicate with nodes. The work of computing nodes in the online visual inspection system is concentrated in two parts: image processing calculation and result feedback. To reduce the impact of communication on computing, the use of asynchronous communication can improve the operating efficiency of parallel systems to a certain extent. According to the division of inspection tasks, determine the number of cameras, industrial control machines, encoders, and other hardware required for inspection, as well as parameters, both parallel ratio and serial ratio. The software connects the detection link to the site's detection environment and links the detection tasks to the corresponding hardware to determine the flow of image processing. After the configuration is completed, the system inspection tasks are executed. To realize the software reconfiguration for product inspection tasks, this paper combines the image processing and evaluation processes into a chain structure, and the flow of the offline configuration and online work of the image inspection chain is shown in Figure 3.

In the system designed in this paper, the calculation nodes communicate directly with the PLC controller, which realizes the local autonomy of the detection function and can effectively minimize the impact of the main program failure. For each computation node error, the main program performs the survival check of the computation node program through the heartbeat mechanism. The main program sends heartbeat packets to the computation node by timing, and the detection program confirms and gives feedback. In this way, the monitoring and alarm of the compute node operation can be realized. Because there are many uncontrollable factors in the factory, on-site equipment and pipelines will bring difficulties to the manual deployment of sensor nodes, so the random deployment of dynamic and static nodes is adopted. The coverage after random deployment and the moving distance of dynamic nodes are two necessary research parameters. To improve the initial coverage and optimize the moving path of dynamic nodes, this paper proposes a mobile deployment optimization scheme based on a probability-aware model. By improving the genetic mutation rules, the ergodicity of the quantum genetic algorithm is improved, thereby improving the initial deployment of the network; the nondestructive testing algorithm is used to optimize the movement path of the dynamic node to the target position.

4. Analysis of Results

4.1. Quantitative Analysis of Detection Models. The effect of the excitation current frequency on the sensitivity of the probe is studied using the probe with the above-determined coil parameters. The current frequency applied to the excitation coil probe is modified during the simulation to obtain and analyze the simulation results. In this simulation, the excitation coil radius is 4 cm, the excitation coil width is 1 cm, the height is 1 cm, the excitation current is 220A, the

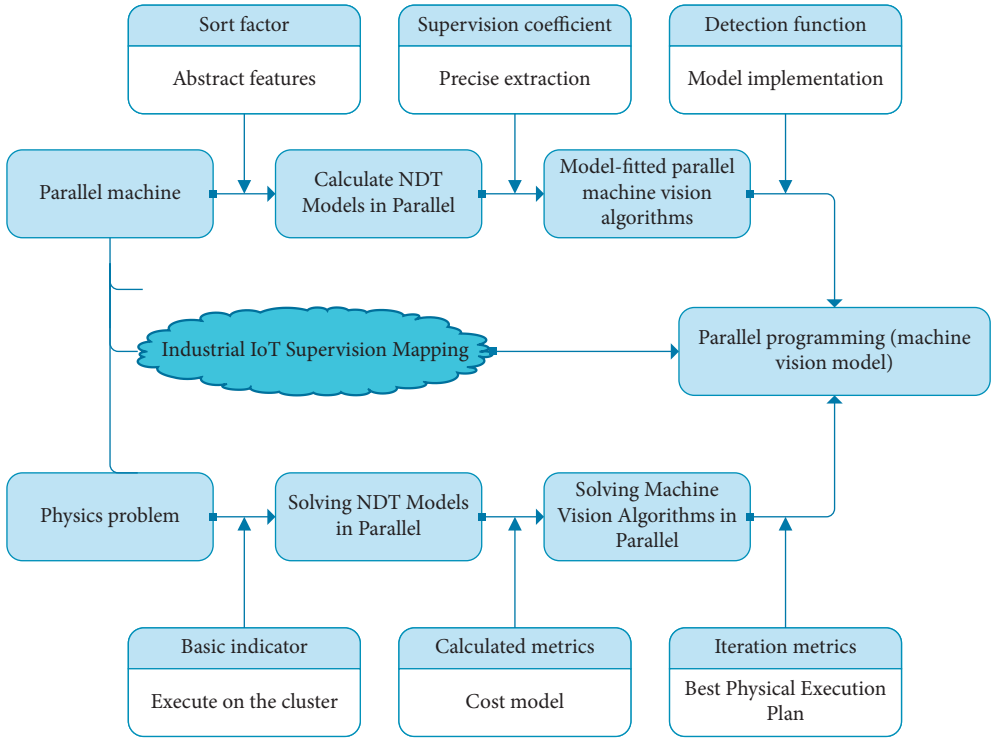

Figure 2: Parallel computing optimization logic.

excitation current frequency is selected from 200 Hz to 5000 Hz, the reference frequency is selected in steps of 100 Hz, a defect of 1 mm in width and 1 mm in depth is detected, and the magnetic induction intensity at the center of the probe is observed. The magnetic induction at the center of the excitation coil with defects is compared with that without defects, the simulation data is extracted, and the sensitivity is calculated in steps of 800 Hz. The obtained data is imported into Origin to obtain the graph of the relationship between excitation current frequency and probe sensitivity as shown in Figure 4. From the graph, it can be inferred that when there are defects on the surface of the aluminum plate, the higher the excitation frequency, the greater the magnetic induction at the center of the observation line, and the greater the sensitivity of the probe. The non-defect detection varies from 0.05 to 0.106, and the defect detection varies from −0.76 to 0.59, which proves that the variation of non-defect detection is more flexible.

The effect of the excitation current level on the sensitivity of the probe is investigated using the probe with the above-determined coil parameters. In the simulation process, current 1 applied to the excitation coil probe is modified to obtain and analyze the simulation results. From Figure 5, it can be seen that in the range of 100–2500 A, the larger the excitation current, the larger the excitation magnetic field, and the larger the eddy current loss in the aluminum plate, so that the magnetic field strength without defects is increasing, the difference between the magnetic induction strength with and without defects is larger, and the sensitivity of the probe is larger. However, in the actual measurement, the equivalent current in the coil cannot be increased indefinitely due to the number of turns of the coil, the input current, and the range of the GMR sensor. In the design of the corresponding eddy current NDT system, the amplitude of the output signal needs to be set with adjustable gain.

4.2. NDT Algorithm Performance Analysis. To verify the optimization performance of the QGA-2 exchange algorithm for node coverage and movement path of hybrid WSNs, MATLAB R2019 software is selected for simulation. Different numbers of dynamic and static hybrid nodes are randomly deployed in a rectangular monitoring area of 400 m × 400 m to measure the optimal number of hybrid nodes to be deployed. The experimental parameters were set as shown in Table 1.

Figure 6 shows the effect of the different numbers of dynamic nodes on coverage improvement for the total number of hybrid nodes of 60, 80, and 100. In the monitoring area, when the number of dynamic nodes is 0, the coverage is improved with the increase of the total number of nodes, and the highest coverage is achieved when 70 hybrid nodes are deployed, with a coverage rate of about 87.15%. 60 hybrid nodes are deployed with an overall lower coverage rate, which cannot meet the coverage requirements. When the total number of hybrid nodes is 80, with 15 to 25 dynamic nodes, the coverage is 95.67%, which is an improvement of about 16.14% compared to the deployment without dynamic nodes. As the number of dynamic nodes increases, the coverage provided by 80 and 100 hybrid nodes is similar and saves network node resources.

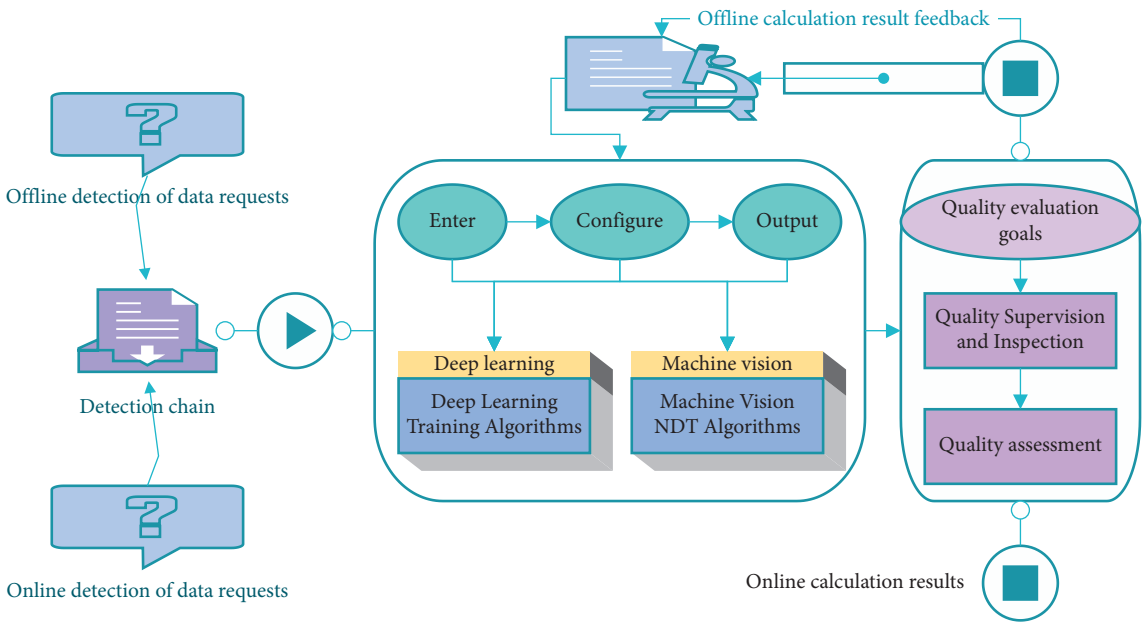

Figure 3: Detection chain workflow.

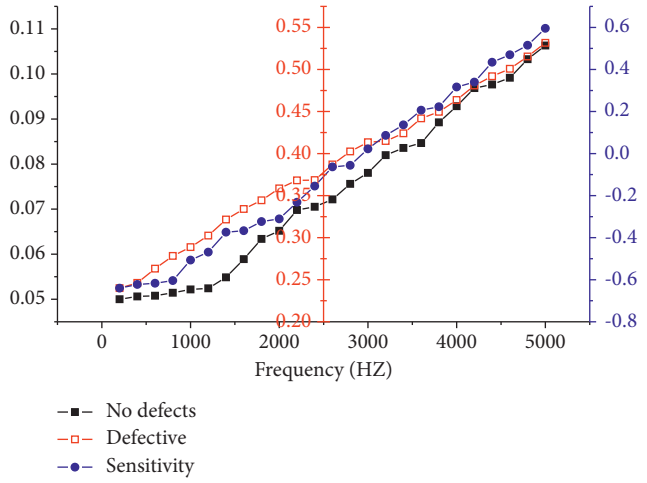

Figure 4: The relationship between excitation current frequency and sensitivity.

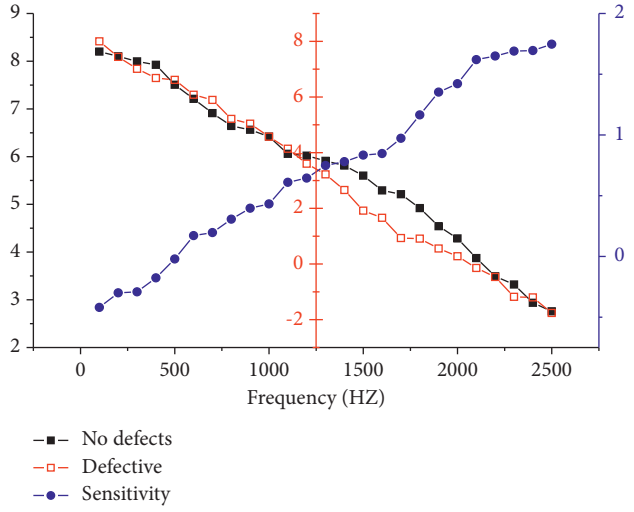

Figure 5: The relationship between excitation current magnitude and probe sensitivity curve.

Table 1: Parameter settings.

Parameter number	Parameter name	Parameter notation	Parameter value
1	Geographic range	P(S)	400 m × 400 m
2	Grid points	N(p)	400 × 400
3	Total number of nodes	T(p)	(60, 80, 100)
4	Monitoring radius	R	40
5	Sensing error	E(s)	8
6	Number of iterations	N(iteration)	500

With 50 static nodes and 10, 20, and 30 dynamic nodes deployed in a specific monitoring area, the coverage of the QGA-2 exchange algorithm is about 8.62%~12.91% higher than that of the cellular structure-based dynamic node optimization in the average moving distance range of 1–50 m, as shown in Figure 7. The dynamic node optimization based on the cellular structure is based on global information processing, which is not easy to fall into the local optimum. After detecting the cavity, the optimal motion path is found, and the increase of dynamic nodes makes the coverage rate improve while the average movement distance decreases. The QGA-2 exchange algorithm optimizes the initial coverage and then exchanges the mobile paths of all dynamic nodes, which further reduces the mobile distance of dynamic nodes.

4.3. Machine Vision NDT System Analysis. The machine vision nondestructive testing of three different array images based on the number of target object images is carried out for the system. The test records of local NDT and machine vision NDT systems were conducted separately to explore the connection between the number of pictures and the efficiency of NDT and further optimize the efficiency of machine vision NDT to improve the efficiency of data acquisition. The specific data are shown in Figure 8(a). The relationship between the number of pictures and the accuracy of NDT was further explored. The specific test results are shown in Figure 8(b).

As can be seen in Figure 8(a), with the increasing number of equipment subjects, the nondestructive detection efficiency of the cloud-based image nondestructive inspection system is higher, with a nondestructive detection rate of about 0.12 s. This is due to the use of EasyAR's CRS module in the design implementation of the machine vision nondestructive inspection system to process the images of the target objects. In the CRS module, a brief and efficient API interface is used to retrieve and track the target images, which enables more accurate and fast finding of the target objects in the real environment. As can be seen from Figure 8(b), the NDT accuracy of the conventional NDT system tends to decrease with the increasing number of NDT objects, while the NDT accuracy of the machine vision NDT system remains at about 99.45%. This shows that the overall stability of the machine vision NDT system in terms of NDT accuracy is good, with little fluctuation.

On the one hand, the machine vision NDT system uses a simple and efficient picture processing interface in the cloud NDT processing module to track and locate the target

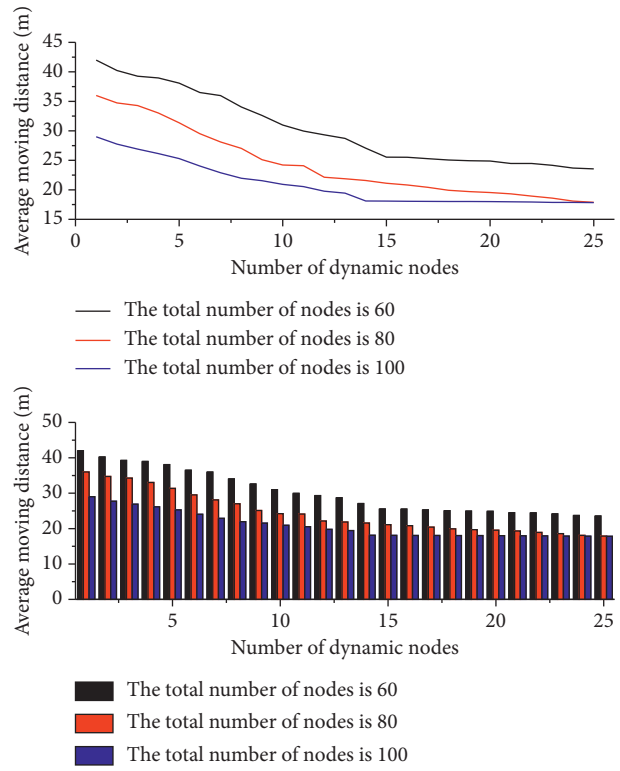

Figure 6: Average moving distance with different numbers of dynamic nodes.

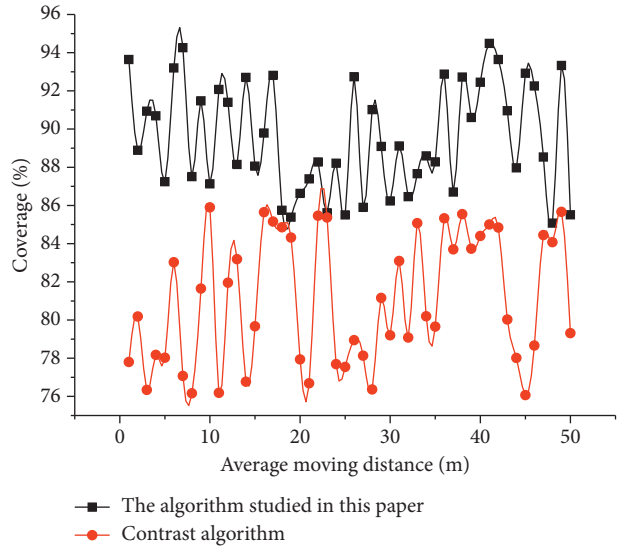

Figure 7: Coverage for different average moving distance ranges.

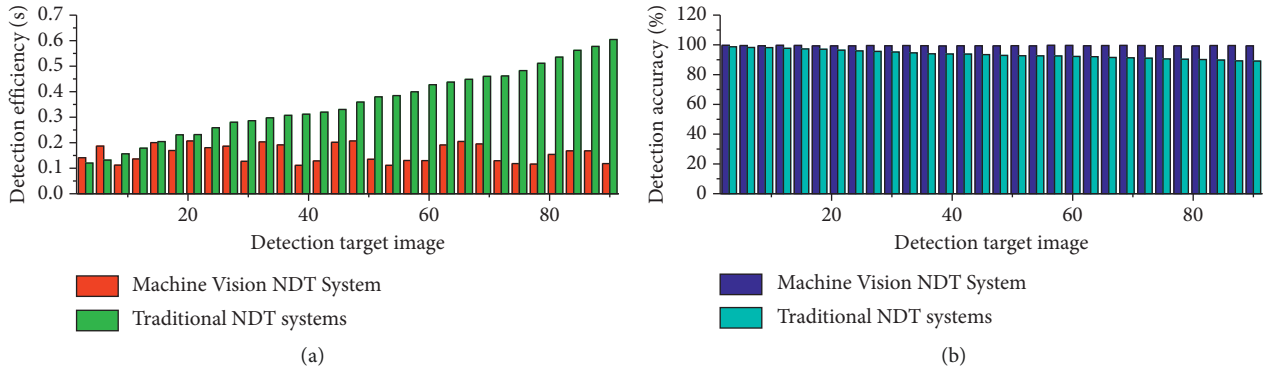

Figure 8: Comparison results of system detection efficiency and accuracy. (a) Detection efficiency comparison results. (b) Detection accuracy comparison results.

pictures of the equipment. On the other hand, as the number of NDT pictures increases, the storage space of mobile devices is affected to a certain extent, which increases the burden of the equipment. The machine vision NDT system uploads the image of the target object to the cloud server, reducing the burden on the equipment. Therefore, the above test results prove that the design and development of the machine vision NDT system can further optimize the nondestructive detection rate of image NDT, improve the efficiency and accuracy of obtaining data information in the industrial IoT, and meet the accuracy requirements of data in manufacturing industry.

5. Conclusion

The paper designs and implements a machine vision nondestructive inspection system based on industrial IoT technology, combining supervision mechanisms, wireless communication technology, communication nondestructive inspection, and cloud server database. The system is not only capable of real-time sensing of industry and data aggregation but also capable of storing data in the cloud server database and presenting it on the display side by calling the data in the database. In response to the coverage voids and incomplete sensing information caused by the random deployment of wireless sensor networks, a hybrid random deployment scheme of dynamic and static nodes is adopted, and the coverage and the movement path of dynamic nodes are optimized using an improved machine vision nondestructive detection algorithm. A sparse NDT model based on a genetic algorithm is designed, which is a hybrid detection model constructed by binary particle swarm algorithm and hidden Markov model; the sparse NDT sample problem is effectively solved by the quality NDT samples expanded by binary particle swarm algorithm; and the quality NDT samples obtained from the expansion are used to estimate the parameters of the hidden Markov-based NDT model. It improves IoT NDT by comparing and analyzing the impact of two NDT models and uses the design of front-end and back-end applications to realize a highly automated and high-precision IoT sparse NDT system. By comparing the detection effect of IoT nondestructive testing through experiments, it is verified that the system has a good detection effect for sparse nondestructive testing of industrial Internet of Things. The big data technology can be applied to the system designed in this paper, and the collected data can be further mined and processed, so that the managers can better grasp the status of the equipment and adjust the production plan at any time to improve the production efficiency and product quality of the enterprise.

Data Availability

The data used to support the findings of this study are available from the corresponding author upon request.

Conflicts of Interest

The authors declare that they have no known competing financial interests or personal relationships that could have appeared to influence the work reported in this paper.

Acknowledgments

This work was supported by the Department of Control Technology, Wuxi Institute of Technology.

References

[1] M. Elbadawi, L. E. McCoubrey, F. K. H. Gavins et al., "Disrupting 3D printing of medicines with machine learning," *Trends in Pharmacological Sciences*, vol. 42, no. 9, pp. 745–757, 2021.

[2] C. C. Cheah, T. Bock, J. Cao et al., "Guest editorial introduction to the focused section on mechatronics and automation for constructions," *IEEE*, vol. 26, no. 6, pp. 2819–2825, 2021.

[3] A. Ghosh and T. Sengupta, "Intello labs: non-destructive digital commodity grading," *Emerging Economies Cases Journal*, vol. 3, no. 1, pp. 51–57, 2021.

[4] D. Rodriguez, M. A. Saed, and C. Li, "A WPT/NFC-based sensing approach for beverage freshness detection using supervised machine learning," *IEEE Sensors Journal*, vol. 21, no. 1, pp. 733–742, 2020.

[5] X. Zhu, A. Mohsin, W. Q. Zaman et al., "Development of a novel noninvasive quantitative method to monitor Siraitia

grosvenorii cell growth and browning degree using an integrated computer-aided vision technology and machine learning," *Biotechnology and Bioengineering*, vol. 118, no. 10, pp. 4092–4104, 2021.

[6] S. F. Wirtz, N. Beganovic, and D. Söffker, "Investigation of damage detectability in composites using frequency-based classification of acoustic emission measurements," *Structural Health Monitoring*, vol. 18, no. 4, pp. 1207–1218, 2019.

[7] M. S. Hossain and H. Taheri, "In-situ process monitoring for metal additive manufacturing through acoustic techniques using wavelet and convolutional neural network (CNN)," *International Journal of Advanced Manufacturing Technology*, vol. 116, no. 11, pp. 3473–3488, 2021.

[8] J. T. C. Liu, A. K. Glaser, K. Bera et al., "Harnessing non-destructive 3D pathology," *Nature Biomedical Engineering*, vol. 5, no. 3, pp. 203–218, 2021.

[9] H. Ding, R. X. Gao, A. J. Isaksson, R. G. Landers, T. Parisini, and Y. Yuan, "State of AI-based monitoring in smart manufacturing and introduction to focused section," *IEEE*, vol. 25, no. 5, pp. 2143–2154, 2020.

[10] L. Chen, X. Yao, P. Xu, S. K. Moon, and G. Bi, "Rapid surface defect identification for additive manufacturing with in-situ point cloud processing and machine learning," *Virtual and Physical Prototyping*, vol. 16, no. 1, pp. 50–67, 2021.

[11] B. Dhiman, Y. Kumar, and Y.-C. Hu, "A general purpose multi-fruit system for assessing the quality of fruits with the application of recurrent neural network," *Soft Computing*, vol. 25, no. 14, pp. 9255–9272, 2021.

[12] S. Khan, Z. Xiaobo, M. Ilyas et al., "Fraud food and food spoilage detection by non-destructive technologies," *Annals of the Romanian Society for Cell Biology*, vol. 25, no. 7, pp. 1389–1405, 2021.

[13] C. K. Sahu, C. Young, and R. Rai, "Artificial intelligence (AI) in augmented reality (AR)-assisted manufacturing applications: a review," *International Journal of Production Research*, vol. 59, no. 16, pp. 4903–4959, 2021.

[14] L. Liu, H. Mei, C. Guo, Y. Tu, and L. Wang, "Pixel-level classification of pollution severity on insulators using photothermal radiometry and multiclass semisupervised support vector machine," *IEEE Transactions on Industrial Informatics*, vol. 17, no. 1, pp. 441–449, 2020.

[15] Z. Zhang, X. Liang, W. Zhao, and L. Xing, "Noise2Context: c," *Medical Physics*, vol. 48, no. 10, pp. 5794–5803, 2021.

[16] D. V. K. Le, Z. Chen, and R. Rajkumar, "Multi-sensors in-line inspection robot for pipe flaws detection," *IET Science, Measurement & Technology*, vol. 14, no. 1, pp. 71–82, 2019.

[17] Q. Sun, M. Zhang, and A. S. Mujumdar, "Recent developments of artificial intelligence in drying of fresh food: a review," *Critical Reviews in Food Science and Nutrition*, vol. 59, no. 14, pp. 2258–2275, 2019.

[18] M. K. Tripathi and D. D. Maktedar, "A role of computer vision in fruits and vegetables among various horticulture products of agriculture fields: a survey," *Information Processing in Agriculture*, vol. 7, no. 2, pp. 183–203, 2020.

[19] A. S. Robles, A. D. J. B. Garcia, J. A. D. D. L. Peña, E. R. Mancera, and N. S. Robles, "The insertion of low-cost additive manufacturing into engineering teaching: a case in central Mexico," *International Journal of Materials and Product Technology*, vol. 59, no. 3, pp. 270–287, 2019.

[20] C. Wu, P. Wu, J. Wang, R. Jiang, M. Chen, and X. Wang, "Critical review of data-driven decision-making in bridge operation and maintenance," *Structure and Infrastructure Engineering*, vol. 18, no. 1, pp. 47–70, 2021.

[21] R. Fotohi and H. Pakdel, "A lightweight and scalable physical layer attack detection mechanism for the internet of things (IoT) using hybrid security schema," *Wireless Personal Communications*, vol. 119, no. 4, pp. 3089–3106, 2021.

[22] M. L. Adekanbi, "Optimization and digitization of wind farms using internet of things : a review," *International Journal of Energy Research*, vol. 45, no. 11, pp. 15832–15838, 2021.